Environmental Pollution 208 (2016) 185–197

Contents lists available at ScienceDirect

Environmental Pollution

journal homepage: www.elsevier.com/locate/envpol

Relationship between rooftop and on-road concentrations of traffic-related pollutants in a busy street canyon: Ambient wind effects

Kyung-Hwan Kwak [a, b], Sang-Hyun Lee [c], Jaemyeong Mango Seo [a], Seung-Bu Park [a, d], Jong-Jin Baik [a, *]

[a] School of Earth and Environmental Sciences, Seoul National University, Gwanak-gu, Seoul 151-742, Republic of Korea
[b] Center for Environment, Health and Welfare Research, Korea Institute of Science and Technology, Seongbuk-gu, Seoul 136-791, Republic of Korea
[c] Department of Atmospheric Science, Kongju National University, Gongju, Chungcheongnam-do 314-701, Republic of Korea
[d] Department of Earth and Environmental Engineering, Columbia University, New York, NY 10027, USA

ARTICLE INFO

Article history:
Received 11 April 2015
Received in revised form
12 July 2015
Accepted 18 July 2015
Available online 30 July 2015

Keywords:
Traffic-related pollutants
Busy street canyon
Ambient wind direction
Rooftop measurement
On-road measurement

ABSTRACT

Rooftop and on-road measurements of O_3, NO_2, NO_x, and CO concentrations were conducted to investigate the relationship between rooftop and on-road concentrations in a busy and shallow street canyon with an aspect ratio of ~0.3 in Seoul, Republic of Korea, from 15 April to 1 May 2014. The median road-to-roof concentration ratios, correlation coefficients between rooftop and on-road concentrations, and temporal variations of rooftop and on-road concentrations are analyzed according to the rooftop wind directions which are two cross-canyon and two along-canyon directions. The analysis results indicate that the relationship is strong when the rooftop is situated on the downwind side rather than on the upwind side. Relative to the cross-canyon wind directions, one of the along-canyon wind directions can more enhance the relationship. A conceptual framework is proposed to explain the effect of ambient wind direction on the relationship between rooftop and on-road concentrations in a street canyon.

1. Introduction

Traffic-related pollutants in urban areas are responsible for adverse health problems (Lipfert et al., 2006; Marshall et al., 2009). Ambient concentrations of traffic-related pollutants have been systematically monitored mainly for regulatory purposes in many countries and have been satisfactorily understood (Clapp and Jenkin, 2001; Pandey et al., 2008; Varotsos et al., 2003). Near-road concentrations of traffic-related pollutants are more directly associated with human exposure issues. However, a roadside air quality monitoring station has a low spatial representativeness of near-road air quality (Berkowicz et al., 1996; Santiago et al., 2013; Scaperdas and Colvile, 1999; Vardoulakis et al., 2005). For example, the spatial extent affected by on-road pollutant emission is known to be within a few hundred meters in the downwind direction from the emission source (Chaney et al., 2011; Kota et al., 2013). Because of the high spatial variability of near-road pollutant concentration in comparison to sparsely distributed roadside air quality monitoring stations, understanding near-road air quality remains poor.

Many commercial and residential buildings are located along a road to form a street canyon. A busy street canyon is frequently regarded as harmful to human health because of the combination of a large traffic volume and its weak ventilation capability (Bagieński, 2015; Kwak and Baik, 2014). Traffic-related pollutant concentrations in a street canyon exhibit very localized features in space and time (Qin and Kot, 1993; Vardoulakis et al., 2011; Weber et al., 2013). Some previous studies have highlighted a strong relationship between indoor and outdoor air quality (Chan, 2002; Lawrence and Fatima, 2014). To better understand air quality in a street canyon and cope with air pollution problems therein, it is necessary to examine air quality at multiple points in a street canyon.

Canyon geometry and on-road emission amount are the important factors determining a relationship between rooftop and on-road pollutant concentrations in a street canyon. Dispersion of traffic-related pollutants in a street canyon of a small canyon aspect ratio (H/W, where H is the building height and W is the width between buildings) is different from that in a street canyon of a large H/W because of different flow regimes (Liu et al., 2011; Oke, 1988). A

* Corresponding author.
E-mail address: jjbaik@snu.ac.kr (J.-J. Baik).

http://dx.doi.org/10.1016/j.envpol.2015.07.030
0269-7491/

busy street canyon that is routinely congested with large traffic volumes is faced with massive emission by vehicles (Carslaw and Beevers, 2004) and experiences a high exposure level to traffic-related pollutants (Kaur et al., 2005). In a street canyon of $H/W = 0.96$ with a traffic volume of approximately 26,000 vehicles day^{-1}, Kukkonen et al. (2001) reported that the road-to-roof NO_2, NO_x, and CO concentration ratios are 1.5, 3.5, and 2.6, respectively. In a deep street canyon of $H/W = 5.7$ with a traffic volume of smaller than 6000 vehicles from 0800 to 2100 LT, the road-to-roof CO concentration ratio is 2.6 from 0000 to 2400 LT and 3.5 from 0700 to 2100 LT, indicating the importance of on-road emission amount from vehicles (Murena and Favale, 2007). In a two-dimensional street canyon of $H/W = 2$, computational fluid dynamics modeling studies have shown that a lower-to-upper concentration ratio is a function of emission rate (Kwak et al., 2013) and exchange velocity (Zhong et al., 2015).

Ambient wind speed and direction are also the important factors determining a relationship between rooftop and on-road pollutant concentrations in a street canyon. The difference between rooftop and on-road particle concentrations in a street canyon of $H/W = 1$ decreases as ambient wind speed increases (Kumar et al., 2009). In contrast, the road-to-roof NO_x concentration ratio in a street canyon of $H/W = 0.55$ tends to increase as ambient wind speed increases (Costabile and Allegrini, 2007). Harrison et al. (2004) showed the importance of ambient wind direction on the relationship between background and roadside particle concentrations. The effect of ambient wind direction on roadside particle concentrations is evident in a street canyon of $H/W \sim 1$ (Kumar et al., 2008). In addition to the cross-canyon wind directions considered by many of the previous studies above, other ambient wind directions such as oblique and along-canyon wind directions need to be considered for examining the relationship between rooftop and on-road concentrations in a street canyon.

This study aims at investigating the relationship between rooftop and on-road concentrations of traffic-related pollutants in a busy street canyon of a small H/W. The distinction of ambient wind direction according to the cross-canyon and along-canyon directions is a suitable methodological approach to explain ambient wind effects on the relationship between rooftop and on-road concentrations. Road-to-roof ratio, correlation coefficient, and temporal change rate are calculated and compared in wind direction classification. In Section 2, measurement site, measurements, and data are described. In Section 3, analysis results are presented and discussed. A summary and conclusions are given in Section 4.

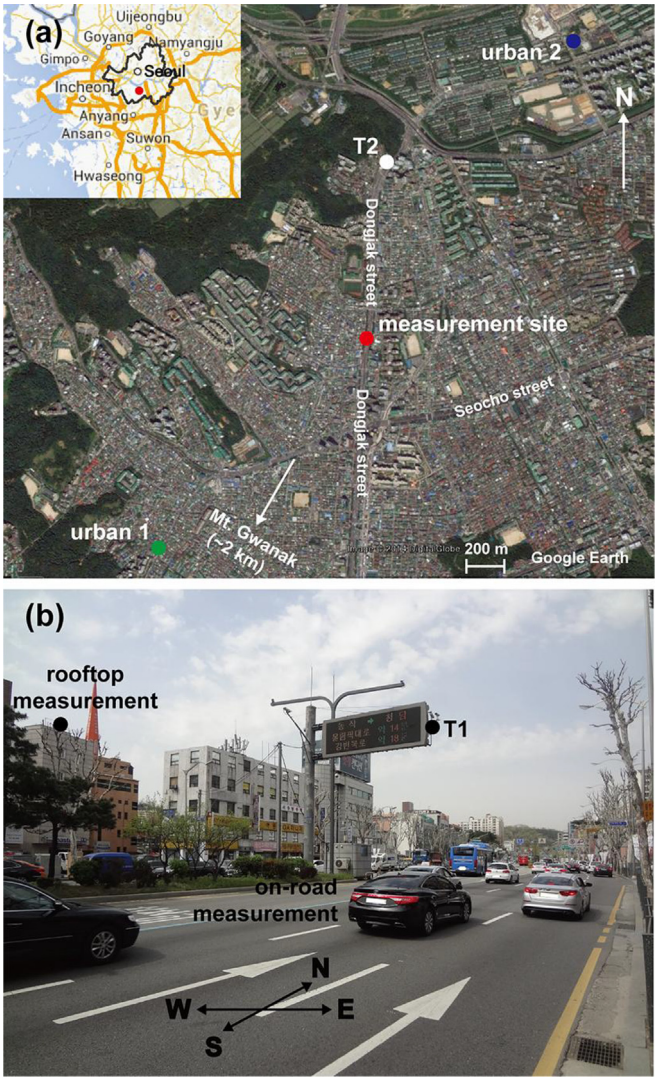

Fig. 1. (a) Satellite image (Google Earth) covering measurement site, traffic count location (T2), and two urban air quality monitoring stations. Inset on the left-top corner is a map of Seoul and its surrounding areas with the measurement site being indicated by a red dot and the boundary of Seoul being indicated by the black solid line. (b) Photo of measurement site showing the rooftop and on-road measurement locations and an automatic traffic-count location (T1).

2. Methodology

2.1. Measurement site

A street canyon with a north-south orientation is located on Dongjak street in a residential area of Seoul, a megacity in Republic of Korea. A largely vegetated area that includes a small mountain is closely located northwest, and Mt. Gwanak with an area of ~19 km^2 and a 632-m elevation at the peak is located southwest (Fig. 1a). The width of the street canyon at the on-road measurement location is 49 m, and the rooftop height of a five-story building where instruments were installed on is 13 m (Fig. 1b). The street canyon of $H/W \sim 0.3$ is characterized as a shallow street canyon. There is no building significantly higher than the five-story building within a radius of ~100 m. Roadside trees are at both sides with an approximately 10-m spacing except for a space in front of the measurement building. The effects of roadside trees on pollutant concentrations can be significant depending on the leaf density (Buccolieri et al., 2009; Gromke and Blocken, 2015; Salmond et al., 2013). Because the measurement was conducted in the early stage of leaf-growing season, the effects of roadside trees are considered to be minor in this study.

Dongjak street has eight lanes including two bus-only lanes in the middle. Because the street is one of the major routes from southern suburban areas to the city center and vice versa, the daily traffic volume excluding motorcycles exceeds 80,000 vehicles regardless of day of a week based on automatic monitoring at T1 in October 2013 (Fig. 2), which is provided by the Seoul Metropolitan Government. The street is routinely congested with large traffic volumes (exceeding 3000 vehicles h^{-1}) from a certain time in the morning to midnight. The maximum hourly traffic volumes were recorded in 0700–0800, 0800–0900, and 1100–1200 LT on weekdays, Saturday, and Sunday, respectively. We confirmed that the diurnal variation in October was almost identical to the diurnal variation in April in traffic volume data at T1. On Wednesday (16 and 23 April 2014), the diurnal variation of traffic volume excluding motorcycles was manually monitored at T2 for this study, which was also similar to that automatically monitored at T1 on weekdays

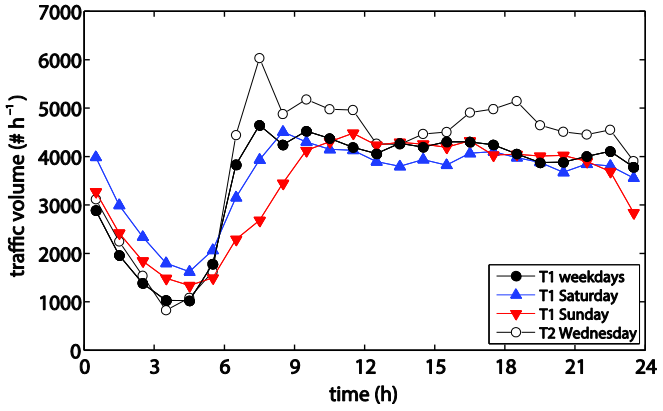

Fig. 2. Diurnal variations of hourly traffic volume at T1 on weekdays, Saturday, and Sunday in October 2013 and at T2 on Wednesday (16 and 23 April 2014).

in October 2013. Therefore, these consistent traffic volumes of approximately 4000 vehicles h^{-1} provide a good opportunity to examine ambient influences on traffic-related pollutant concentrations rather than the influence of on-road emission.

2.2. Measurements and data

O_3, NO_x, and CO concentrations were measured from 15 April to 1 May 2014 using ultraviolet absorption O_3 analyzers, chemiluminescence NO_x analyzers, and infrared absorption CO analyzers, respectively. Table 1 provides an overview of the instruments installed at the measurement site (rooftop and on-road) and two urban air quality monitoring stations. At the rooftop, O_3, NO_x, and CO analyzers and a weather station (wind speed and direction sensors and an air temperature sensor) were installed during the measurement period for this study. The three analyzers with lower detectable limits of <0.4 ppb (O_3), 0.4 ppb (NO_x), and 0.04 ppm (CO) were initially calibrated on-site on 14 April before starting measurements. The NO_x and CO analyzers were additionally calibrated due to a technical problem and restarted on 21 April. The rooftop NO_x concentrations during the period of 22 April–1 May (10 days) are used for the analysis. Because of another technical problem of the CO analyzer occurred at 2120 LT on 27 April, the rooftop CO concentrations during the period of 22–27 April (6 days) are used for the analysis. At the end of measurement period, data screening is performed. Some abnormal data that are $NO_x \geq 300$ ppb and $NO \geq 200$ ppb (0.14%) at the rooftop are excluded from the analysis. A weather station powered by a solar panel was installed 4 m higher than the three analyzers to prevent biased data caused by rooftop obstacles. Rooftop wind speed and direction and air temperature were recorded every second at the weather station. At the on-road and two urban air quality monitoring stations, O_3, NO_x, and CO concentrations and wind speed and direction are routinely measured and managed by the Korean Ministry of Environment following the protocol for the air quality monitoring operation guide and regulations (Air Korea). During the 17-day period, the hourly-averaged concentrations have 2, 0, and 4 abnormal data out of 408 at the on-road, 'urban 1', and 'urban 2' air quality monitoring stations, respectively. The abnormal data are not used for the analysis.

Table 1
Overview of instruments at the (a) rooftop and (b) on-road locations and (c, d) two urban air quality monitoring stations.

Variable	Model	Data interval	Period	Precision
a) Rooftop				
O_3	Teledyne T400	10 min	15 April–1 May	<0.5%
NO_x, NO, NO_2	Teledyne T200	10 min	22 April–1 May	0.5%
CO	Teledyne T300	10 min	22–27 April	0.5%
WS, WD[a]	Onset S-WSA-M003	1 s	15 April–1 May	4%
	Onset S-WDA-M003	1 s	15 April–1 May	5°
T_a[b]	Onset S-TMB-M002	1 s	15 April–1 May	0.2 °C
b) On-road				
O_3	Horiba APOA-370	1 h	15 April–1 May	1%
NO_x, NO, NO_2	Horiba APNA-370	1 h	15 April–1 May	1%
CO	Horiba APMA-370	1 h	15 April–1 May	1%
WS, WD[a]	Youngjun UWS-200	1 h	15 April–1 May	3%, 3°
c) Urban 1				
O_3	Kimoto OA-683	1 h	15 April–1 May	n.a.[c]
NO_x, NO, NO_2	Kimoto NA-623	1 h	15 April–1 May	n.a.[c]
CO	Kimoto ZRF	1 h	15 April–1 May	n.a.[c]
d) Urban 2				
O_3	Horiba APOA-370	1 h	15 April–1 May	1%
NO_x, NO, NO_2	Horiba APNA-370	1 h	15 April–1 May	1%
CO	Horiba APMA-370	1 h	15 April–1 May	1%

[a] WS, WD: wind speed and direction.
[b] T_a: air temperature.
[c] n.a.: not available.

Based on the street-canyon orientation, the rooftop location is upwind for westerly winds and downwind for easterly winds. In the post-processing, the rooftop wind speed and direction are converted into horizontal wind components in the east-west (i.e., cross-canyon) and north-south (i.e., along-canyon) directions at every second and then averaged over every hour. Although the rooftop wind speed in 1-s intervals has a low accuracy, the hourly-averaged wind speed is reliably considered to be the ambient wind speed compared to the average wind speed at the two urban air quality monitoring stations ($R^2 = 0.76$). The hourly rooftop wind speed (WS_r) and direction (WD_r) are calculated using the hourly-averaged horizontal wind components. When $WS_r \geq 0.3$ m s^{-1}, winds blowing from $45° \leq WD_r < 135°$, from $135° \leq WD_r < 225°$, from $225° \leq WD_r < 315°$, and from $0° \leq WD_r < 45°$ or $315° \leq WD_r < 360°$ are classified into easterly, southerly, westerly, and northerly winds, respectively. When $WS_r < 0.3$ m s^{-1}, the wind direction classification is not made. Then, the hourly concentration data are classified according to easterly ($N = 46$), southerly ($N = 21$), westerly ($N = 52$), and northerly ($N = 46$) winds from 22 April to 1 May.

3. Results and discussion

3.1. Overall description

Fig. 3 shows the time series of rooftop air temperature and ambient, rooftop, and on-road O_3, NO_2, NO_x, and CO concentrations from 15 April to 1 May. The rooftop air temperature generally exhibits a typical diurnal variation in the springtime except for rainy days exhibiting noticeably irregular variations. There were four rainy days on 17, 27, 28, and 29 April with daily rainfall amounts of 3.0, 8.5, 14.5, and 4.5 mm, respectively, at the nearest automatic weather station. The rooftop O_3 concentration is much higher than the on-road O_3 concentration and comparable to the ambient O_3 concentrations. The highest rooftop O_3 concentration typically occurs in the afternoon, whereas the highest rooftop O_3 concentration occurs at night on 27, 28, and 29 April, which are rainy days. The highest daily maximum of rooftop O_3 concentration occurs on 23 April followed by 25 and 24 April, which are clear and sunny days. The rooftop concentrations of primary pollutants (i.e., NO_2, NO_x, and CO) are much lower than the on-road concentrations and quite similar to the ambient concentrations. During the 10-day period from 22 April to 1 May, the primary pollutant concentrations tend to be higher on clear and sunny days than on rainy days, which is primarily due to different synoptic-scale meteorological conditions.

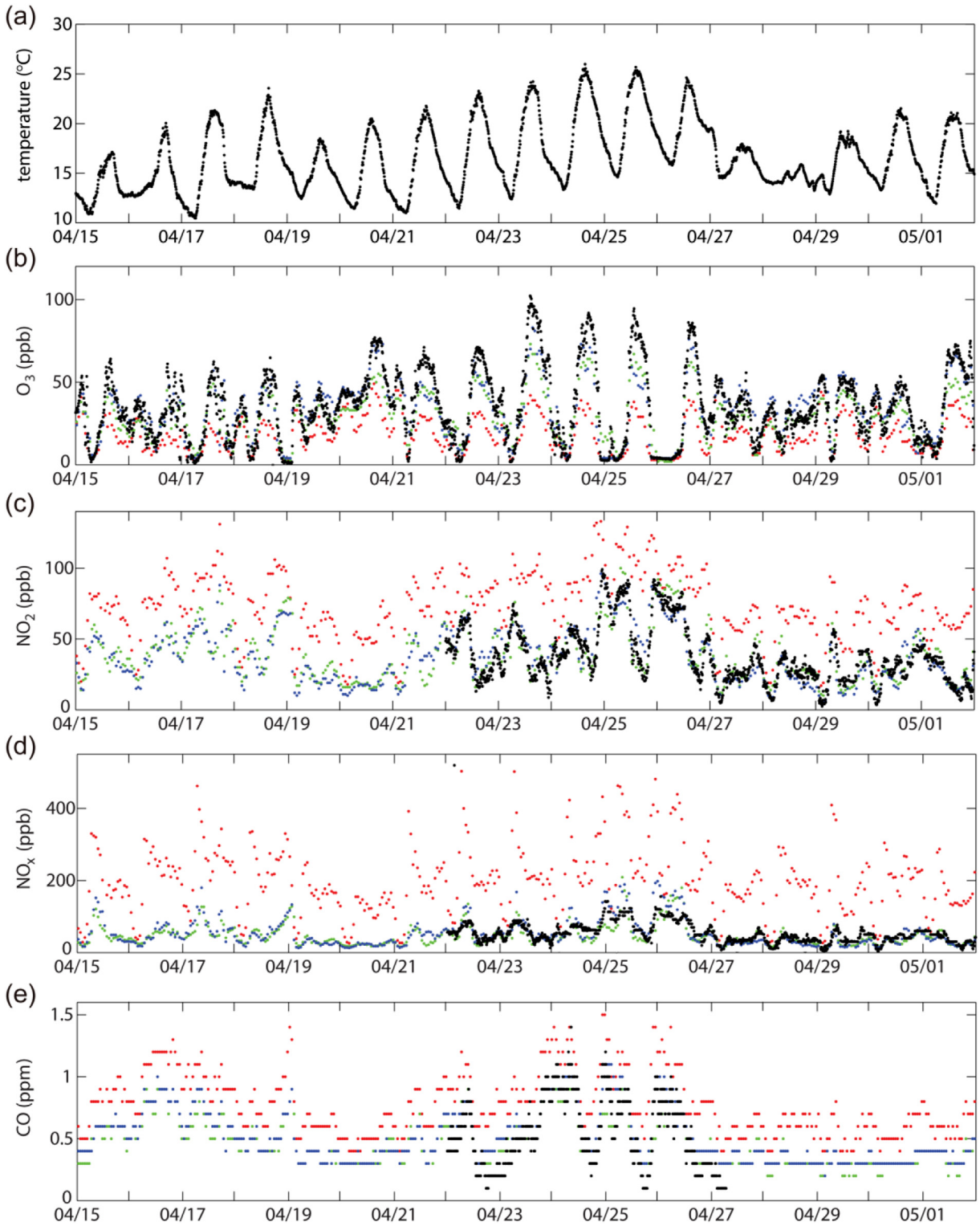

Fig. 3. Time series of (a) rooftop air temperature and rooftop (black), on-road (red), two ambient (green for urban 1, blue for urban 2) (b) O_3, (c) NO_2, (d) NO_x, and (e) CO concentrations.

Rooftop wind speed and direction approximately representing ambient meteorological conditions are shown as a wind-rose diagram (Fig. 4a). At the rooftop location, two predominant wind directions are found during the 17-day period. On clear and sunny days, winds blowing from the south-to-west with wind speeds lower than 2 m s^{-1} are apparent. Westerly winds are frequently characterized as sea breezes from the west coast in the afternoon (Park et al., 2015). On rainy days, winds predominantly blow from the northeast-to-east with wind speeds occasionally exceeding 2 m s^{-1} (8%). The on-road wind directions are predominantly along-canyon directions regardless of the rooftop wind directions (Fig. 4b). The along-canyon wind directions in a street canyon are

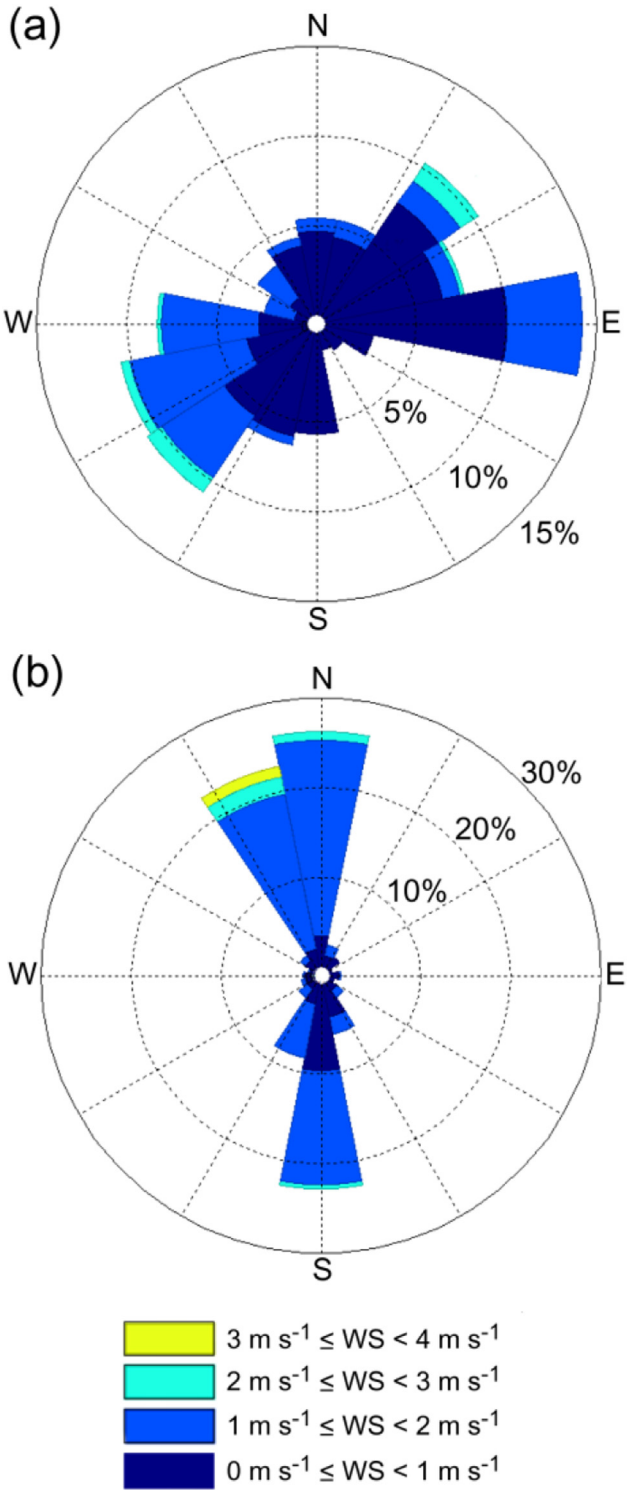

Fig. 4. Wind-rose diagrams at the (a) rooftop and (b) on-road locations during the 17-day period.

attributed to channeling flows which are observed when the rooftop wind directions are oblique and parallel to the street-canyon orientation (Boddy et al., 2005; Park et al., 2015; Tomlin et al., 2009) and also traffic-induced flows in the driving directions on the street (Kastner-Klein et al., 2001). Interestingly, the average on-road wind speed (1.3 m s^{-1}) is 1.4 times higher than the average rooftop wind speed (0.9 m s^{-1}). The higher on-road wind speed is evident at times when the rooftop wind speed is below 1 m s^{-1} (i.e., at night and in the morning), and this is due to traffic-induced flows and turbulence especially in the two bus-only lanes that are adjacent to the on-road air quality monitoring station (Longley et al., 2004a,b).

Fig. 5 shows the diurnal variations of air temperature and wind speed (velocity components) at the rooftop location and the diurnal variations of O_3, NO_2, NO_x, and CO concentrations at the four different locations. The highest rooftop air temperature and wind speed occur in the late afternoon (i.e., 1540 and 1700 LT, respectively). The cross-canyon component of rooftop wind maximized at 1740 LT is eastward from 1250 LT. The along-canyon component of rooftop wind is mostly southward in the daytime and northward in the nighttime, while the temporal variation is less apparent for the along-canyon component than for the cross-canyon component. The highest and lowest O_3 concentrations occur in 1400–1600 and 0600–0800 LT, respectively. The highest rooftop O_3 concentration (60 ppb) is higher than the highest ambient (47 and 53 ppb) and on-road (29 ppb) concentrations. The higher rooftop O_3 concentration relative to the ambient O_3 concentrations in the afternoon can be a result of O_3 transport by northwesterly to westerly winds from the largely vegetated area regarded as intra-urban sources of biogenic O_3 precursors (Wagner and Kuttler, 2014). The NO_2, NO_x, and CO concentrations have two major peaks in the morning and at night. The rooftop and ambient concentrations of the primary pollutants are relatively low in the afternoon due to enhanced mixing in the developed urban boundary layer. On the other hand, the on-road NO_2 concentration remains relatively high in the afternoon. This is because the on-road NO_2 concentration is mainly determined by on-road NO_x emission and subsequent chemical conversion from NO to NO_2.

3.2. Road-to-roof concentration ratios

The relationship between rooftop and on-road concentrations of traffic-related pollutants is obviously associated with pollutant dispersion in a street canyon and is basically associated with ambient wind speed and ambient wind direction relative to a street-canyon orientation. In this study, a traditional estimation method, the road-to-roof concentration ratio, is used to represent the relationship between rooftop and on-road concentrations. Table 2 summarizes and compares the road-to-roof concentration ratios reported in the literature. The median (mean ± standard deviation) road-to-roof concentration ratios are 0.53 (0.56 ± 0.18) for O_3, 2.1 (2.4 ± 1.0) for NO_2, 4.2 (4.4 ± 1.9) for NO_x, and 1.8 (2.2 ± 1.0) for CO for all wind directions, which are approximately similar to or smaller than the concentration ratios for NO_2, NO_x, and CO and larger than the concentration ratio for O_3 measured at a street canyon in Lahti, Finland (Väkevä et al., 1999). The road-to-roof NO_x and CO concentration ratios are apparently larger on the upwind side than on the downwind side in a street canyon of $H/W = 1.1$ (Xie et al., 2003). The similar road-to-roof O_3 concentration ratio (0.58) was recently reported for a busy street canyon of Seoul (Park et al., 2015).

The road-to-roof O_3, NO_2, NO_x, and CO concentration ratios classified according to the five rooftop wind speed classifications are shown in box plots (Fig. 6). Among the five rooftop wind speed classifications, the smallest median road-to-roof concentration ratios of NO_2 (1.59) and CO (1.60) and the largest median road-to-roof concentration ratio of O_3 (0.64) are consistently found for the classification of rooftop wind speed <0.3 m s^{-1}. In comparison to the classifications of rooftop wind speed >1.0 m s^{-1}, the median road-to-roof concentration ratios are consistently smaller for NO_2, NO_x, and CO and larger for O_3 for the classifications of rooftop wind speed <1.0 m s^{-1}. The road-to-roof O_3, NO_2, NO_x, and CO

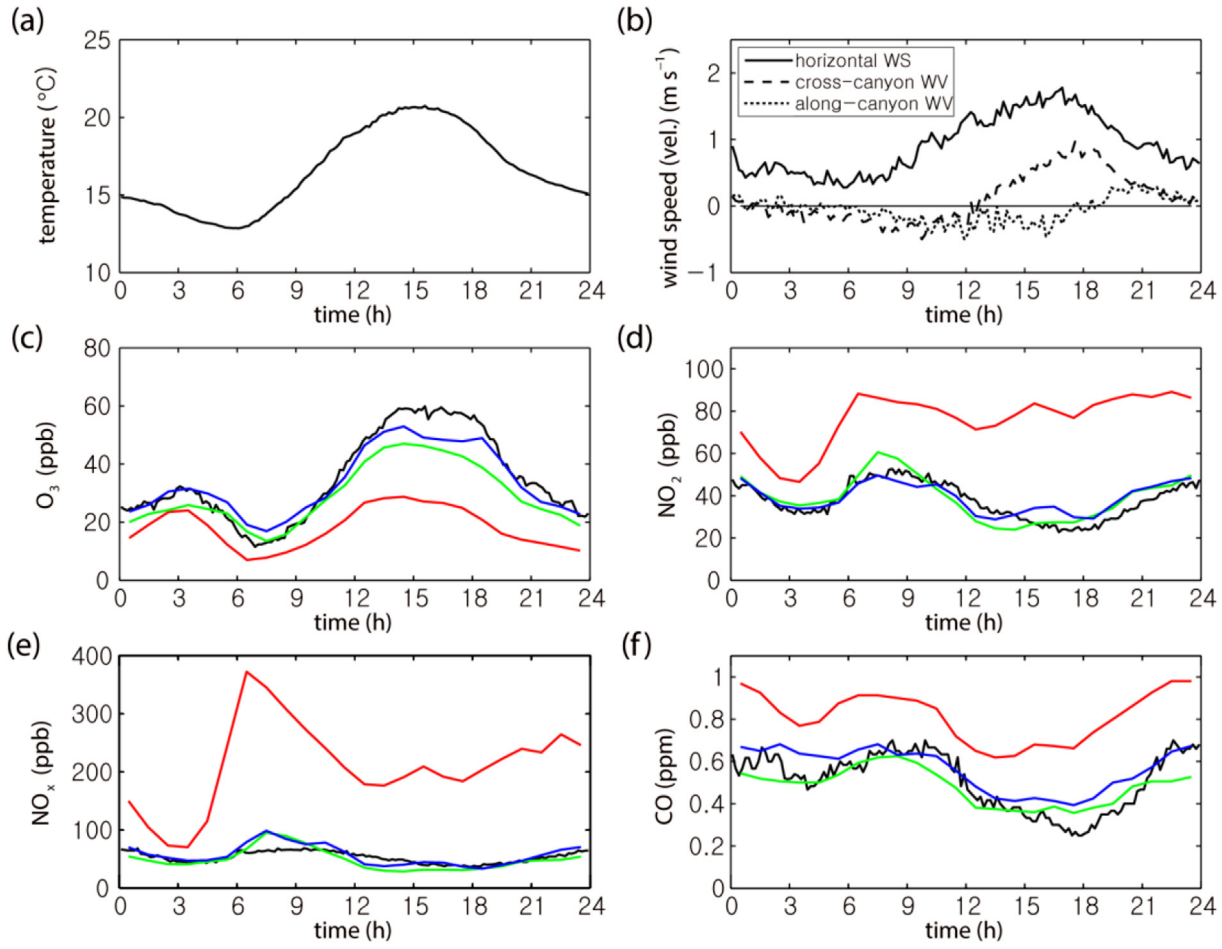

Fig. 5. Diurnal variations of rooftop (a) air temperature and (b) wind speed (velocity components), and rooftop (black), on-road (red), two ambient (green for urban 1, blue for urban 2) (c) O_3, (d) NO_2, (e) NO_x, and (f) CO concentrations. In (b), positive values of cross-canyon and along-canyon velocity components refer to eastward and northward components, respectively. The air temperature, wind speed (velocity components), and O_3 concentration are fitted for the 17-day period; the NO_2 and NO_x concentrations are fitted for the 10-day period; the CO concentrations are fitted for the 6-day period.

concentration ratios classified according to the four rooftop wind directions are shown in box plots (Fig. 7). The smallest median road-to-roof concentration ratios of NO_2 (1.94), NO_x (3.69), and CO (1.62) are consistently found for southerly winds. Considering the rooftop wind speeds >0.3 m s^{-1}, the variations of median road-to-roof NO_2, NO_x, O_3, and CO concentration ratios among the four rooftop wind directions are obviously larger than those among the four rooftop wind speed classifications. The statistical significance of differences among the four rooftop wind directions is confirmed by performing the analysis of variance (ANOVA), showing that *p*-values of road-to-roof O_3, NO_2, and NO_x concentration ratios are ~10^{-7}, ~10^{-7}, and 0.07, respectively (the number of road-to-roof CO concentration ratio for each rooftop wind direction is not sufficient for performing the ANOVA). As a result, the relationship between rooftop and on-road concentrations of traffic-related pollutants in the busy and shallow street canyon is more significantly influenced by the rooftop wind direction than by the rooftop wind speed. In addition, the relationship is stronger for one of the along-canyon wind directions (i.e., southerly winds) rather than for cross-canyon wind directions regarding the road-to-roof concentration ratios.

The O_3, NO_2, NO_x, and CO concentrations classified according to

Table 2
Comparisons of reported road-to-roof concentration ratios.

	Road-to-roof concentration ratio				Site	Period	*H*/*W*
	O_3	NO_2	NO_x	CO			
This study	0.53	2.1	4.2	1.8	Seoul	2014.4.22.–5.1	0.3
Väkevä et al. (1999)	0.12	2.1	4.9	5.1	Lahti	1995.9.4–20	n.a.[a]
Kukkonen et al. (2001)	–	1.5	3.5	2.6	Helsinki	1997.3.3–4.30	1.0
Xie et al. (2003)	0.85	3.2	4.8	4.1	Guangzhou	1999.7.18–24	1.1
	0.55	1.2	1.7	1.4		1999.10.12–18	
Murena and Favale (2007)	–	–	–	2.6	Naples	2006.6.14–20	5.7
Park et al. (2015)	0.58	–	–	–	Seoul	2013.6.25–27	n.a.[a]

[a] n.a.: not available.

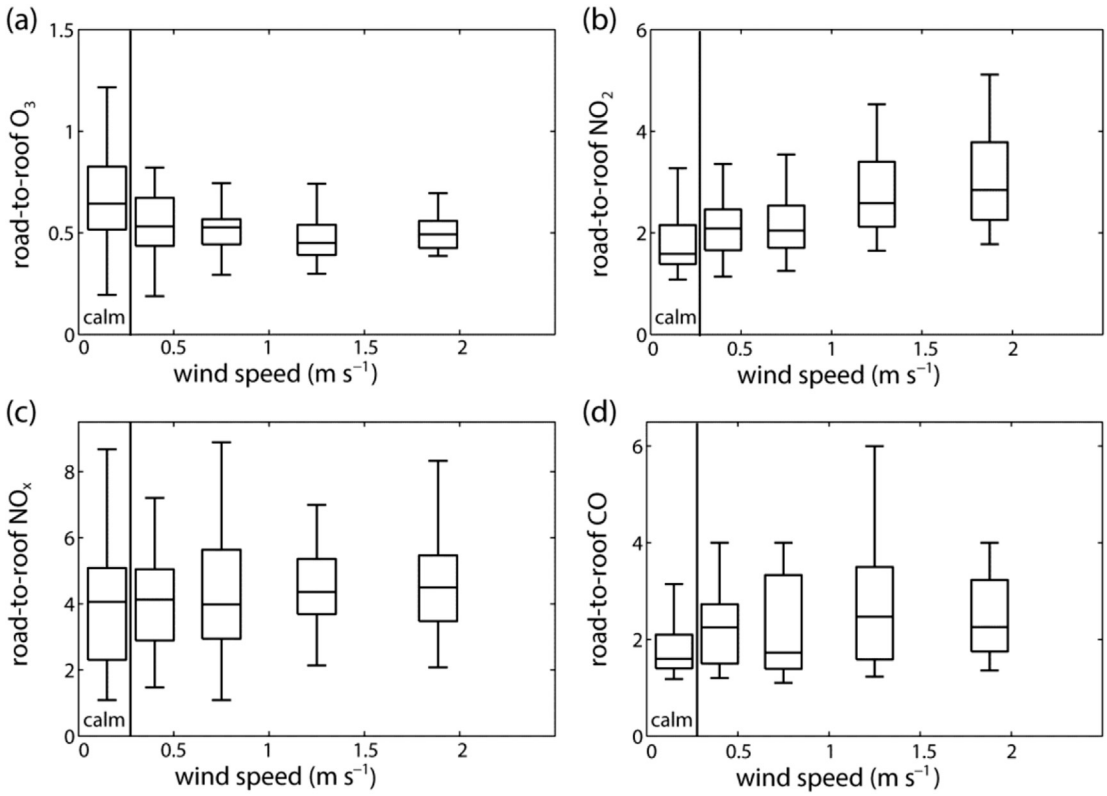

Fig. 6. Box plots of road-to-roof (a) O_3, (b) NO_2, (c) NO_x, and (d) CO concentration ratios as a function of hourly rooftop wind speed (WS_r). The road-to-roof concentration ratios are classified into five wind speed classifications ($WS_r < 0.3$ m s^{-1}, 0.3 m $s^{-1} \leq WS_r < 0.5$ m s^{-1}, 0.5 m $s^{-1} \leq WS_r < 1.0$ m s^{-1}, 1.0 m $s^{-1} \leq WS_r < 1.5$ m s^{-1}, and $WS_r \geq 1.5$ m s^{-1}).

the four rooftop wind directions are shown in box plots (Fig. 8a, b, c, and e). Note that the on-road concentrations are less variable among the four rooftop wind directions compared to the ambient and rooftop concentrations because of the dominant influence of on-road emission on the on-road concentrations. The rooftop exposures to NO_2, NO_x, and CO at typical ranges of on-road

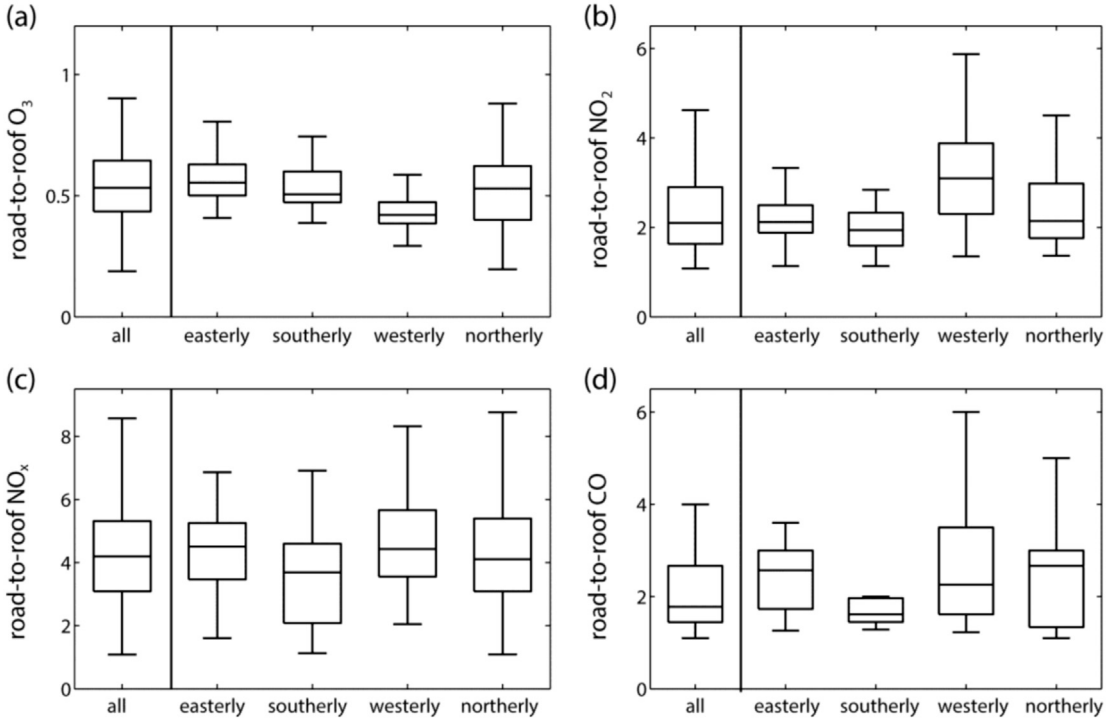

Fig. 7. Box plots of road-to-roof (a) O_3, (b) NO_2, (c) NO_x, and (d) CO concentration ratios as a function of hourly rooftop wind direction. The road-to-roof concentration ratios are classified into five wind direction classifications (all, easterly, southerly, westerly, and northerly winds).

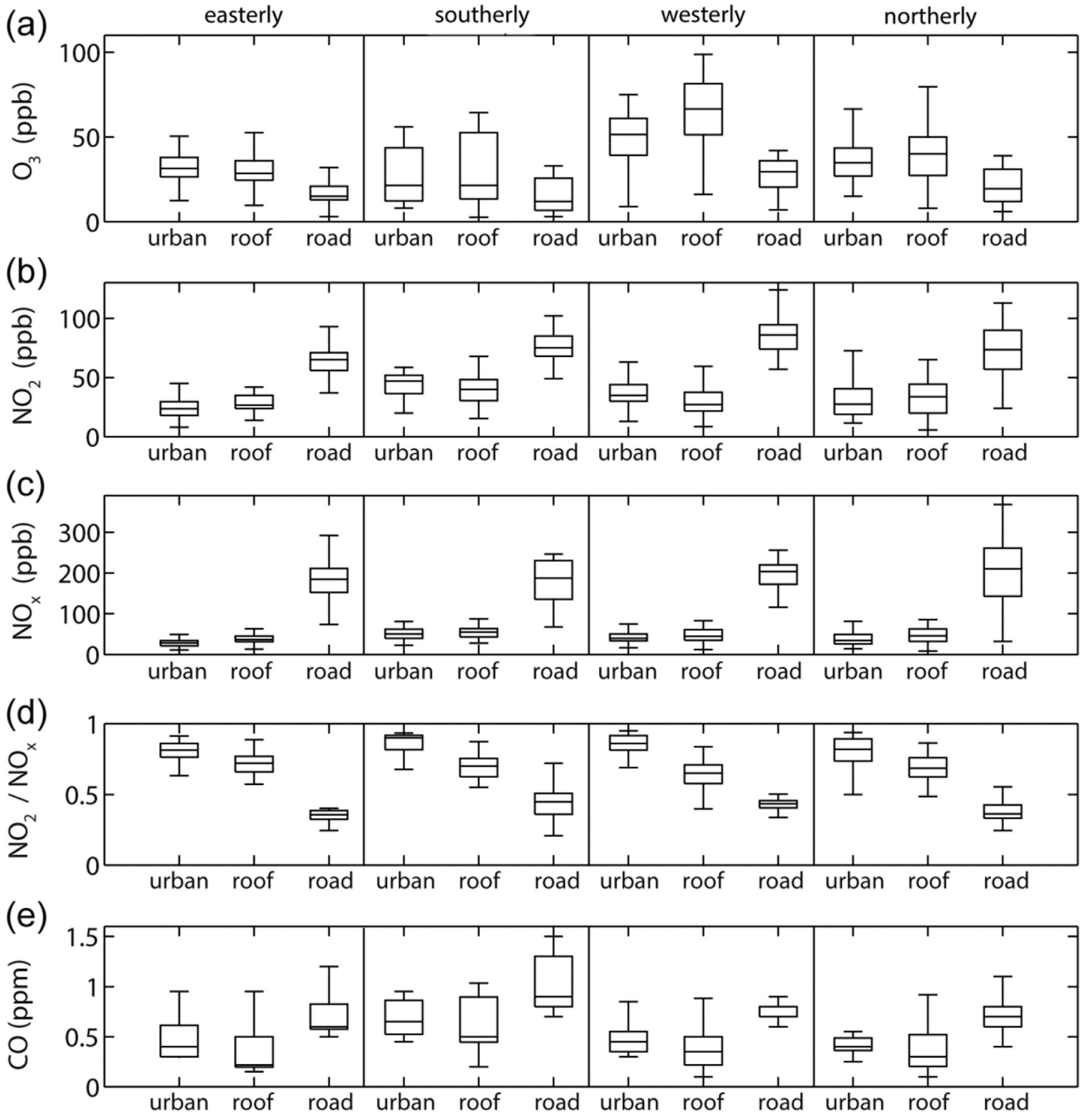

Fig. 8. Box plots of ambient, rooftop, and on-road (a) O_3, (b) NO_2, (c) NO_x, and (e) CO concentrations and (d) NO_2-to-NO_x concentration ratio classified according to four rooftop wind directions. The ambient concentrations are the average concentrations at two urban air quality monitoring stations.

concentrations are estimated using the percentiles of box plots. Here, a range from 25th to 75th percentiles of on-road concentrations is considered as a typical range. From 22 April to 1 May, 14%, 0%, and 30% of the rooftop NO_2, NO_x, and CO concentrations, respectively, correspond to typical or even higher on-road concentrations for all rooftop wind directions. The highest frequencies of rooftop exposure to typical or even higher on-road concentrations (12% for NO_2, 3% for NO_x, and 37% for CO) are consistently found for southerly winds. This suggests the significance of along-canyon wind direction in pollutant dispersion, which was raised by Soulhac and Salizzoni (2010) through analytical and numerical modeling in an idealized street canyon. On the other hand, the lowest frequencies (1% for NO_2, 0% for NO_x, and 7% for CO) are consistently found for westerly winds. These results imply that the rooftop exposure to the primary pollutants is worsened for southerly winds and alleviated for westerly winds prevailing especially in the afternoon on clear and sunny days.

The NO_2-to-NO_x concentration ratio shown in Fig. 8d informs whether air at a location is relatively fresh or polluted (Kwak et al., 2013). A typical NO_2-to-NO_x concentration ratio of emitted air from

vehicles on roads is as large as 0.28 in Seoul (Shon et al., 2011). The rooftop NO_2-to-NO_x concentration ratio is mostly between the ambient and on-road ratios. The rooftop NO_2-to-NO_x concentration ratios smaller than the ambient ratios reveal the less-aged air at the rooftop location compared to that at the urban air quality monitoring stations, implying that the rapid chemical conversion from NO to NO_2 is the determining process of NO_x-O_3 composition in the street canyon.

3.3. Correlations and temporal variations

The correlations between rooftop and on-road pollutant concentrations for the four rooftop wind directions are shown in Fig. 9, and their coefficients are listed in Table 3. In the scatter diagrams, the rooftop and on-road O_3 concentrations are well correlated with a slope larger for westerly winds than for the other wind directions, whereas the NO_2 and NO_x concentrations are more scattered. The O_3 and CO correlation coefficients (0.90 and 0.90, respectively) are larger than the NO_2 and NO_x correlation coefficients (0.69 and 0.59, respectively). These correlation coefficients are similar to the O_3, NO, NO_2, and CO correlation coefficients of 0.63–0.81 reported by Väkevä et al. (1999) and higher than the O_3 correlation coefficient of 0.73 reported by Costabile and Allegrini (2007). The large variations of correlation coefficients indicate the substantial influence of rooftop wind direction on the relationship between rooftop and on-road concentrations. The largest NO_2, NO_x, and CO correlation coefficients are consistently found for easterly winds. For easterly winds, the on-road primary pollutants appear to be directly transported toward the downwind direction in the shallow street canyon.

Table 3
O_3, NO_2, NO_x, and CO correlation coefficients between rooftop and on-road concentrations for all and four different rooftop wind directions based on the linear regression ($y = Ax + B$).

	All	Easterly	Southerly	Westerly	Northerly
O_3	0.90	0.93	0.97	0.87	0.77
NO_2	0.69	0.83	0.71	0.55	0.74
NO_x	0.59	0.68	0.41	0.50	0.60
CO	0.90	0.98	0.88	0.82	0.82

The temporal variation of rooftop concentration is obviously related to that of on-road concentration as well as that of ambient concentration. As shown in Figs. 2 and 5, the temporal variation of

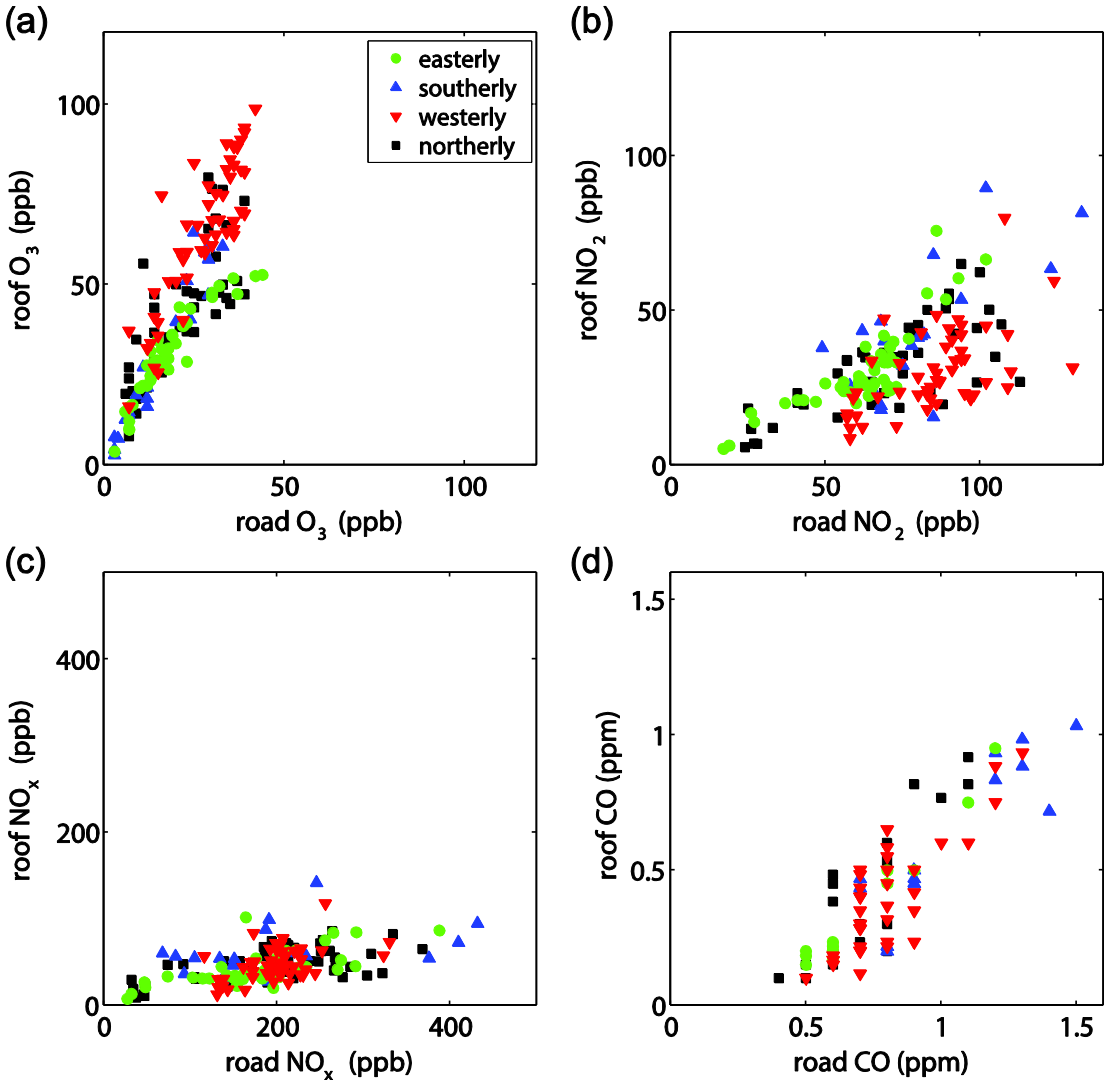

Fig. 9. Scatter diagrams between rooftop and on-road (a) O_3, (b) NO_2, (c) NO_x, and (d) CO concentrations for easterly (green circle), southerly (blue triangle), westerly (red reverse triangle), and northerly (black square) winds.

on-road concentration is dominantly determined by that of traffic volume corresponding to on-road emission amount. In this study, the direct influence of pollutant dispersion from on-road sources at the rooftop location is quantitatively estimated by comparing the temporal change rates of rooftop and on-road pollutant concentrations. For example, if the rooftop concentration increases (decreases) at a time of decreasing (increasing) on-road concentration, the rooftop concentration can be interpreted to be more influenced by ambient factors than on-road emission amount.

Fig. 10 shows the scatter diagrams of hourly change rates between rooftop and on-road concentrations of O_3 and NO_x for the four rooftop wind directions. As expected from the strong correlation between rooftop and on-road O_3 concentrations (Table 3), many of hourly change rates of rooftop and on-road O_3 concentrations have the same sign. For all wind directions, only 22 out of 237 (9%) exhibit opposite signs (Table 4). This indicates that dominant factors influencing the rooftop and on-road O_3 concentrations are consistently the ambient factors. On the contrary, the hourly change rates of rooftop and on-road NO_x concentrations frequently have opposite signs, which are 109 out of 237 (46%) for all wind directions (Table 4). The highest percentages of inconsistency of the sign of hourly change rates between rooftop and on-road O_3 and NO_x concentrations (17% and 60%, respectively) are found for westerly winds (Table 4). In Fig. 10c, the negative correlation coefficient of hourly change rates between rooftop and on-road NO_x concentrations for westerly winds indicates that dominant factors influencing the rooftop and on-road NO_x concentrations are normally inconsistent for westerly winds.

Here are two contrasting examples, which are out-of-phase and in-phase temporal variations of rooftop and on-road concentrations, demonstrating the effect of rooftop wind direction on the relationship between rooftop and on-road NO_x concentrations (Fig. 11). From 1200 LT on 23 April to 0600 LT on 24 April, which was in the middle of clear and sunny days, rooftop winds are predominantly westerly and occasionally weak southerly (Fig. 11a). Following the temporal variation of traffic volume, the on-road NO_x concentration remains at approximately 200 ppb until midnight on 23 April and is lower than 100 ppb from 0100 to 0400 LT on 24 April. On the other hand, the rooftop NO_x concentration exhibits two local maxima that correspond to the local minima of on-road NO_x concentration at approximately 2000 LT on 23 April and 0200 LT on 24 April. As a result, the temporal variations of rooftop and on-road NO_x concentrations are approximately out of phase, which indicates the weakened relationship between rooftop and on-road NO_x concentrations under the influence of westerly winds. From 1800 LT on 27 April to 1200 LT on 28 April, which was in the middle of rainy days, rooftop winds are always easterly with wind speeds of occasionally lower than 0.3 m s^{-1} (Fig. 11b). Morning and

Table 4
Frequencies of opposite signs of hourly change rates between rooftop and on-road concentrations of O_3 and NO_x for all and four different rooftop wind directions.

	All	Easterly	Southerly	Westerly	Northerly
O_3	9%	7%	0%	17%	12%
	22/237	3/42	0/23	9/53	5/41
NO_x	46%	31%	35%	60%	46%
	109/237	13/42	8/23	32/53	19/41

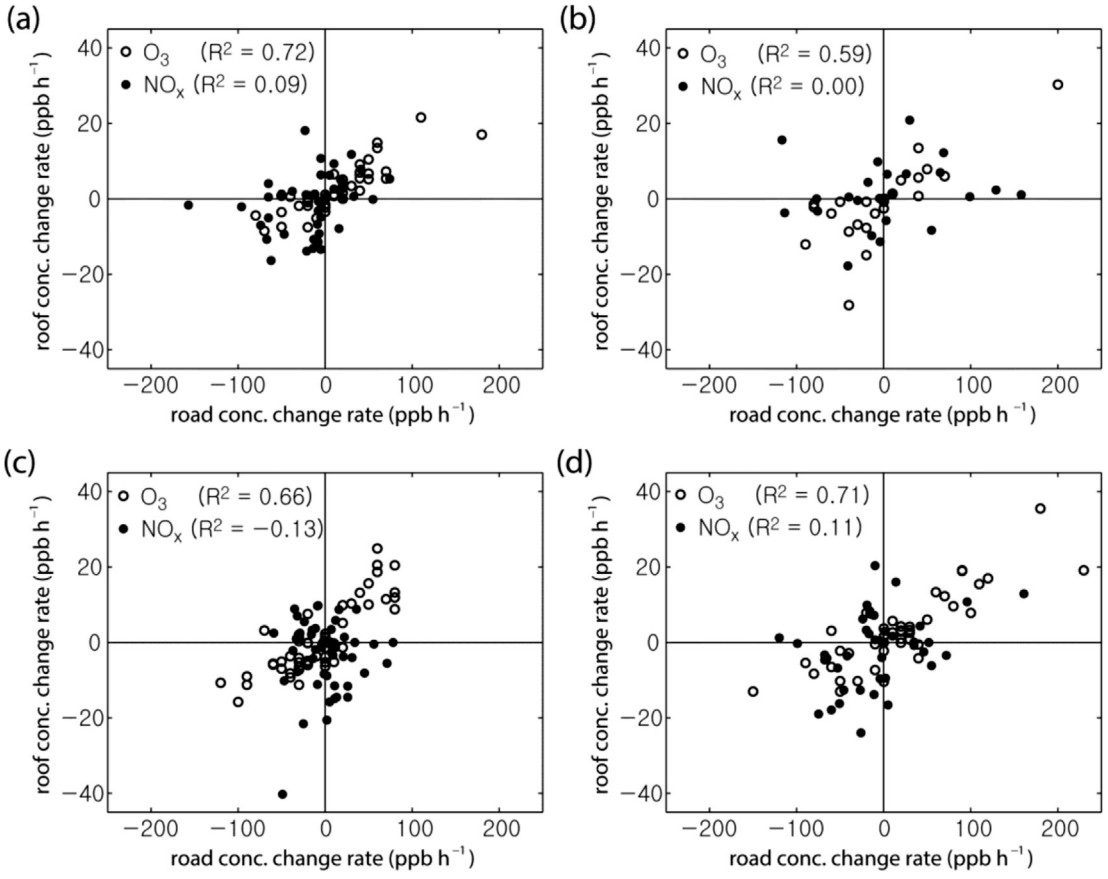

Fig. 10. Scatter diagrams of hourly change rates between rooftop and on-road concentrations of O_3 (open circle) and NO_x (closed circle) for (a) easterly, (b) southerly, (c) westerly, and (d) northerly winds. The O_3 and NO_x correlation coefficients are calculated based on the linear regression ($y = A'x$).

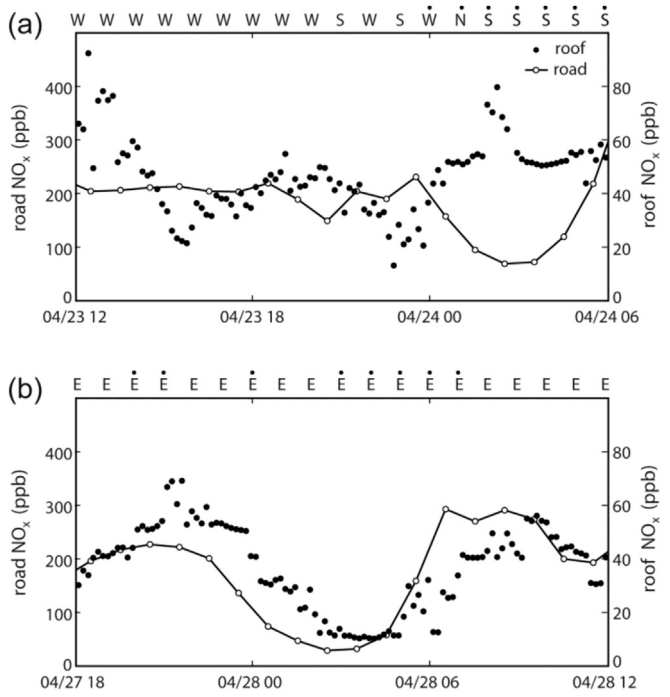

Fig. 11. Time series of rooftop (closed circle) and on-road (solid line with open circle) NO_x concentrations (a) from 1200 LT on 23 April to 0600 LT on 24 April and (b) from 1800 LT on 27 April to 1200 LT on 28 April. Rooftop wind directions are denoted on the top of panels. Dotted letters are the classification of rooftop wind speed <0.3 m s^{-1}.

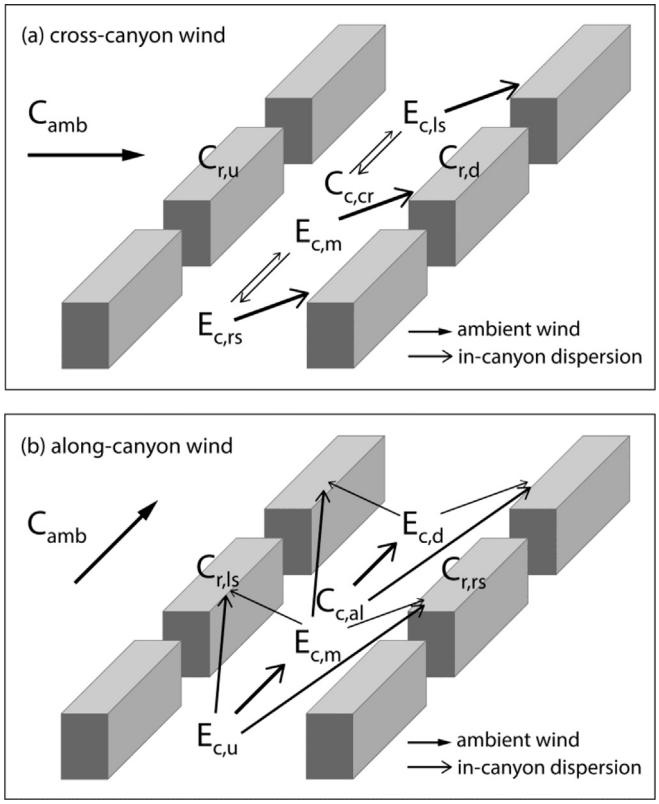

Fig. 12. Schematics of in-canyon pollutant dispersion processes for (a) cross-canyon and (b) along-canyon wind directions. The width of arrows indicates the relative importance of dispersion processes.

evening maxima and a nighttime minimum are consistently found at the rooftop and on-road locations. As a result, the temporal variations of rooftop and on-road NO_x concentrations are apparently in phase with a slight time lag, which indicates the enhanced relationship between rooftop and on-road NO_x concentrations under the influence of easterly winds.

3.4. Conceptual framework

Based on the results presented above, a conceptual framework is proposed to explain the relationship between rooftop and on-road concentrations of traffic-related pollutants. Fig. 12 depicts schematics of in-canyon pollutant dispersion processes for cross-canyon and along-canyon wind directions at a given canyon aspect ratio (e.g., $H/W \sim 0.3$ in this study). For cross-canyon wind directions, the upwind and downwind rooftop concentrations ($C_{r,u}$ and $C_{r,d}$, respectively) and the on-road concentration ($C_{c,cr}$) are expressed as

$$C_{r,u} = C_{amb}, \tag{1}$$

$$C_{r,d} = C_{amb} + f_{r,cr}(E_{c,m}), \tag{2}$$

$$C_{c,cr} = C_{amb} + f_{c,cr}(E_{c,m}, E_{c,rs}, E_{c,ls}), \tag{3}$$

where C_{amb} is the ambient concentration and $E_{c,m}$, $E_{c,rs}$, and $E_{c,ls}$ are the on-road emission rates at the middle, right-side, and left-side locations, respectively. The upwind rooftop concentration is not a function of on-road emission rate, whereas the downwind rooftop concentration is a function of on-road emission rate at the middle location. The relationship between the rooftop concentration and the on-road emission rate depending on a wind direction confirms (i) the largest NO_2, NO_x, and CO correlation coefficients for easterly winds, (ii) the highest percentages of inconsistency of the sign of hourly change rates between rooftop and on-road O_3 and NO_x concentrations for westerly winds, and (iii) the out-of-phase and in-phase temporal variations of rooftop and on-road NO_x concentrations for westerly and easterly winds, respectively. For along-canyon wind directions, the rooftop concentrations at the right-side and left-side locations ($C_{r,rs}$ and $C_{r,ls}$, respectively) and the on-road concentration ($C_{c,al}$) are expressed as

$$C_{r,rs} = C_{r,ls} = C_{amb} + f_{r,al}(E_{c,m}, E_{c,u}), \tag{4}$$

$$C_{c,al} = C_{amb} + f_{c,al}(E_{c,m}, E_{c,u}), \tag{5}$$

where $E_{c,u}$ is the on-road emission rate at the upwind location. If the on-road emission rate is ideally the same along the street canyon orientation (i.e., $E_{c,u} = E_{c,m}$), the rooftop and on-road concentrations would show a concurrent variation for the two along-canyon wind directions. However, the results show that the NO_2, NO_x, and CO correlation coefficients for southerly and northerly winds are lower than those for easterly winds. Instead, the median road-to-roof NO_2, NO_x, and CO concentration ratios are the smallest for southerly winds but not for northerly winds, implying that the on-road emission rate at the upwind location for southerly winds is frequently higher than that at the middle location (i.e., $E_{c,u} > E_{c,m}$). The unexpectedly higher on-road emission rate at the upwind location for southerly winds can be attributed to the large intersection with two crossing subway lines at a 450-m distance southward from the measurement site (Fig. 1a). Three-dimensional numerical modeling techniques such as a computational fluid dynamics modeling are suitable for further examining the relationship between rooftop and on-road concentrations of traffic-related pollutants depending on ambient wind direction.

4. Summary and conclusions

The rooftop and on-road concentrations of traffic-related pollutants (i.e., O_3, NO_2, NO_x, and CO) were measured in a busy street canyon with a north-south orientation in Seoul from 15 April to 1 May 2014. Regardless of day of a week, the street is routinely congested with traffic from a certain time in the morning to midnight. The pollutant concentrations measured at two urban air quality monitoring stations are also taken into account for comparison to the rooftop and on-road concentrations. The rooftop O_3 concentrations are significantly higher than the on-road O_3 concentrations, whereas the rooftop NO_2, NO_x, and CO concentrations are significantly lower than the on-road NO_2, NO_x, and CO concentrations. Because ambient wind direction is important for pollutant dispersion in a street canyon, we classify the measurement data according to the four rooftop wind directions (i.e., easterly, southerly, westerly, and northerly) that are two cross-canyon and two along-canyon directions. Firstly, the smallest road-to-roof NO_2, NO_x, and CO concentration ratios are found for southerly winds. Secondly, the lowest frequencies of rooftop exposure to typical or higher on-road concentrations of the primary pollutants are found for westerly winds. Thirdly, the largest NO_2, NO_x, and CO correlation coefficients between rooftop and on-road concentrations are found for easterly winds. Finally, the temporal variations of rooftop and on-road NO_x concentrations are more likely to be out of phase for westerly winds but in phase for easterly winds.

Consequently, the relationship between rooftop and on-road concentrations in the street canyon is consistently stronger for easterly winds (i.e., the rooftop location on the downwind side) than for westerly winds (i.e., the rooftop location on the upwind side) between the cross-canyon wind directions. This is in line with the results of previous studies focusing on pollutant dispersion in typical street canyons for cross-canyon wind directions. It is interesting that ambient winds with one of the along-canyon wind directions can enhance the relationship between rooftop and on-road concentrations in the busy and shallow street canyon compared to those with one of the cross-canyon wind directions. A proposed conceptual framework explains that the enhanced relationship for one of the along-canyon wind directions is attributed to a higher emission rate at the upwind location than at the measurement site. Because the effect of ambient winds on the rooftop and on-road concentrations of traffic-related pollutants is not confined in two dimensions in actual street and building geometries, the effect of various ambient wind directions should be considered in air quality research and management.

Acknowledgments

The authors are grateful to two anonymous reviewers for providing valuable comments on this work. This work was supported by the National Research Foundation of Korea (NRF) grant funded by the Korea Ministry of Science, ICT and Future Planning (MSIP) (No. 2011-0017041) and the NIMR/KMA R&D program “Integrated Weather Services for Urban and Rural Area” (3133-302-210-13).

References

Air Korea, 2014. http://www.airkorea.or.kr/airkorea/eng/.
Bagieński, Z., 2015. Traffic air quality index. Sci. Total Environ. 505, 606–614.
Berkowicz, R., Palmgren, F., Hertel, O., Vignati, E., 1996. Using measurements of air pollution in streets for evaluation of urban air quality — meteorological analysis and model calculations. Sci. Total Environ. 189–190, 259–265.
Boddy, J.W.D., Smalley, R.J., Dixon, N.S., Tate, J.E., Tomlin, A.S., 2005. The spatial variability in concentrations of a traffic-related pollutant in two street canyons in York, UK — part I: the influence of background winds. Atmos. Environ. 39, 3147–3161.
Buccolieri, R., Gromke, C., Di Sabatino, S., Ruck, B., 2009. Aerodynamics effects of trees on pollutant concentration in street canyons. Sci. Total Environ. 407, 5247–5256.
Carslaw, D.C., Beevers, S.D., 2004. Investigating the potential importance of primary NO_2 emissions in a street canyon. Atmos. Environ. 38, 3585–3594.
Chan, A.T., 2002. Indoor–outdoor relationships of particulate matter and nitrogen oxides under different outdoor meteorological conditions. Atmos. Environ. 36, 1543–1551.
Chaney, A.M., Cryer, D.J., Nicholl, E.J., Seakins, P.W., 2011. NO and NO_2 interconversion downwind of two different line sources in suburban environments. Atmos. Environ. 45, 5863–5871.
Clapp, L.J., Jenkin, M.E., 2001. Analysis of the relationship between ambient levels of O_3, NO_2 and NO as a function of NO_x in the UK. Atmos. Environ. 35, 6391–6405.
Costabile, F., Allegrini, I., 2007. Measurements and analyses of nitrogen oxides and ozone in the yard and on the roof of a street-canyon in Suzhou. Atmos. Environ. 41, 6637–6647.
Google Earth, 2014. http://www.google.com/earth/.
Gromke, C., Blocken, B., 2015. Influence of avenue-trees on air quality at the urban neighborhood scale. Part II: traffic pollutant concentrations at pedestrian level. Environ. Pollut. 196, 176–184.
Harrison, R.M., Jones, A.M., Barrowcliffe, R., 2004. Field study of the influence of meteorological factors and traffic volumes upon suspended particle mass at urban roadside sites of differing geometries. Atmos. Environ. 38, 6361–6369.
Kastner-Klein, P., Fedorovich, E., Rotach, M.W., 2001. A wind tunnel study of organised and turbulent air motions in urban street canyons. J. Wind Eng. Ind. Aerodyn. 89, 849–861.
Kaur, S., Nieuwenhuijsen, M.J., Colvile, R.N., 2005. Pedestrian exposure to air pollution along a major road in Central London, UK. Atmos. Environ. 39, 7307–7320.
Kota, S.H., Ying, Q., Zhang, Y., 2013. Simulating near-road reactive dispersion of gaseous air pollutants using a three-dimensional Eulerian model. Sci. Total Environ. 454–455, 348–357.
Kukkonen, J., Valkonen, E., Walden, J., Koskentalo, T., Aarnio, P., Karppinen, A., et al., 2001. A measurement campaign in a street canyon in Helsinki and comparison of results with predictions of the OSPM model. Atmos. Environ. 35, 231–243.
Kumar, P., Fennell, P., Britter, R., 2008. Effect of wind direction and speed on the dispersion of nucleation and accumulation mode particles in an urban street canyon. Sci. Total Environ. 402, 82–94.
Kumar, P., Fennell, P.S., Hayhurst, A.N., Britter, R.E., 2009. Street versus rooftop level concentrations of fine particles in a Cambridge street canyon. Bound.-Layer Meteorol. 131, 3–18.
Kwak, K.-H., Baik, J.-J., Lee, K.-Y., 2013. Dispersion and photochemical evolution of reactive pollutants in street canyons. Atmos. Environ. 70, 98–107.
Kwak, K.-H., Baik, J.-J., 2014. Diurnal variation of NO_x and ozone exchange between a street canyon and the overlying air. Atmos. Environ. 86, 120–128.
Lawrence, A., Fatima, N., 2014. Urban air pollution & its assessment in Lucknow City — the second largest city of North India. Sci. Total Environ. 488–489, 447–455.
Lipfert, F.W., Wyzga, R.E., Baty, J.D., Miller, J.P., 2006. Traffic density as a surrogate measure of environmental exposures in studies of air pollution health effects: long-term mortality in a cohort of US veterans. Atmos. Environ. 40, 154–169.
Liu, C.-H., Cheng, W.C., Leung, T.C.Y., Leung, D.Y.C., 2011. On the mechanism of air pollutant re-entrainment in two-dimensional idealized street canyons. Atmos. Environ. 45, 4763–4769.
Longley, I.D., Gallagher, M.W., Dorsey, J.R., Flynn, M., Barlow, J.F., 2004a. Short-term measurements of airflow and turbulence in two street canyons in Manchester. Atmos. Environ. 38, 69–79.
Longley, I.D., Gallagher, M.W., Dorsey, J.R., Flynn, M., Bower, K.N., Allan, J.D., 2004b. Street canyon aerosol pollutant transport measurements. Sci. Total Environ. 334–335, 327–336.
Marshall, J.D., Brauer, M., Frank, L.D., 2009. Healthy neighborhoods: walkability and air pollution. Environ. Health Perspect. 117, 1752–1759.
Murena, F., Favale, G., 2007. Continuous monitoring of carbon monoxide in a deep street canyon. Atmos. Environ. 41, 2620–2629.
Oke, T.R., 1988. Street design and urban canopy layer climate. Energy Build. 11, 103–113.
Pandey, S.K., Kim, K.-H., Chung, S.-Y., Cho, S.-J., Kim, M.-Y., Shon, Z.-H., 2008. Long-term study of NO_x behavior at urban roadside and background locations in Seoul, Korea. Atmos. Environ. 42, 607–622.
Park, S.-B., Kwak, K.-H., Han, B.-S., Ganbat, G., Lee, H., Seo, J.M., et al., 2015. Measurements of turbulent flow and ozone at rooftop and sidewalk sites in a high-rise building area. Sci. Online Lett. Atmos. 11, 1–4.
Qin, Y., Kot, S.C., 1993. Dispersion of vehicular emission in street canyons, Guangzhou city, South China (P.R.C.). Atmos. Environ. 27B, 283–291.
Salmond, J.A., Williams, D.E., Laing, G., Kingham, S., Dirks, K., Longley, I., et al., 2013. The influence of vegetation on the horizontal and vertical distribution of pollutants in a street canyon. Sci. Total Environ. 443, 287–298.
Santiago, J.L., Martín, F., Martilli, A., 2013. A computational fluid dynamic modelling approach to assess the representativeness of urban monitoring stations. Sci. Total Environ. 454–455, 61–72.
Scaperdas, A., Colvile, R., 1999. Assessing the representativeness of monitoring data from an urban intersection site in Central London, UK. Atmos. Environ. 33, 661–674.
Shon, Z.-H., Kim, K.-H., Song, S.-K., 2011. Long-term trend in NO_2 and NO_x levels and

their emission ratio in relation to road traffic activities in East Asia. Atmos. Environ. 45, 3120–3131.
Soulhac, L., Salizzoni, P., 2010. Dispersion in a street canyon for a wind direction parallel to the street axis. J. Wind Eng. Ind. Aerodyn. 98, 903–910.
Tomlin, A.S., Smalley, R.J., Tate, J.E., Barlow, J.F., Belcher, S.E., Arnold, S.J., et al., 2009. A field study of factors influencing the concentrations of a traffic-related pollutant in the vicinity of a complex urban junction. Atmos. Environ. 43, 5027–5037.
Väkevä, M., Hämeri, K., Kulmala, M., Lahdes, R., Ruuskanen, J., Laitinen, T., 1999. Street level versus rooftop concentrations of submicron aerosol particles and gaseous pollutants in an urban street canyon. Atmos. Environ. 33, 1385–1397.
Vardoulakis, S., Gonzalez-Flesca, N., Fisher, B.E.A., Pericleous, K., 2005. Spatial variability of air pollution in the vicinity of a permanent monitoring station in central Paris. Atmos. Environ. 39, 2725–2736.
Vardoulakis, S., Solazzo, E., Lumbreras, J., 2011. Intra-urban and street scale variability of BTEX, NO_2 and O_3 in Birmingham, UK: implications for exposure assessment. Atmos. Environ. 45, 5069–5078.
Varotsos, C.A., Efstathiou, M.N., Kondratyev, K.Y., 2003. Long-term variation in surface ozone and its precursors in Athens, Greece — a forecasting tool. Environ. Sci. Pollut. Res. 10, 19–23.
Wagner, P., Kuttler, W., 2014. Biogenic and anthropogenic isoprene in the near-surface urban atmosphere — a case study in Essen, Germany. Sci. Total Environ. 475, 104–115.
Weber, S., Kordowski, K., Kuttler, W., 2013. Variability of particle number concentration and particle size dynamics in an urban street canyon under different meteorological conditions. Sci. Total Environ. 449, 102–114.
Xie, S., Zhang, Y., Qi, L., Tang, X., 2003. Spatial distribution of traffic-related pollutant concentrations in street canyons. Atmos. Environ. 37, 3213–3224.
Zhong, J., Cai, X.-M., Bloss, W.J., 2015. Modelling the dispersion and transport of reactive pollutants in a deep urban street canyon: using large-eddy simulation. Environ. Pollut. 200, 42–52.